

Research Article

Ecological risk and pollution assessment of heavy metals in Jubail coastal sediments, Arabian Gulf: A multiscale assessment

Majed A. Almalki^a, Hassan Y. Alfaifi^{a,b,*}, Khalid N. Alharbi^c, Mubarak M. Albarqi^c, Raed A. Alsulami^c, Sarah H. Alqahtani^c, Musaad K. Aleid^d, Hany M. Almotairy^e

^aNational Aquatic Science Research Laboratory, King Abdulaziz City for Science and Technology, Riyadh, Saudi Arabia

^bInstitute of Waste Management and Recycling Technology, King Abdulaziz City for Science and Technology, Riyadh, Saudi Arabia

^cNuclear Science Research Institute, King Abdulaziz City for Science and Technology, Riyadh, Saudi Arabia

^dInstitute of Water Management and Treatment Technologies, King Abdulaziz City for Science and Technology, Riyadh, Saudi Arabia

^eSaudi Food and Drug Authority, Saudi Food and Drug Authority, Riyadh, Saudi Arabia

ARTICLE INFO

Keywords:

Anthropogenic enrichment
Bioaccumulation pathways
Ecological risk assessment
Metal concentrations
Multivariate statistical analysis
Potential ecological risk index
Pollution load index

ABSTRACT

Industrialization along the Arabian Gulf coast has intensified concerns about heavy metal (HM) accumulation in marine sediments, yet comprehensive site-based ecological assessments remain limited. This study investigates the distribution, contamination levels, and ecological risks of HMs and metalloids in 32 surface seabed sediments collected from offshore, midshore, and inshore zones around Jubail City, Saudi Arabia. Using a combination of geochemical indices (CF, EF, Igeo, PLI, and PERI) and multivariate analysis (PCA), the study distinguishes between lithogenic background inputs and anthropogenic sources associated with industrial discharge, port activities, and desalination outfalls. Results show that most metals were within global background levels. PCA results revealed two dominant controlling factors: a natural component (Fe, Mn, Cr, Ni) and an anthropogenic one (Cd, As, Cu, Zn). Pollution Load Index (PLI) suggested low to moderate contamination near industrial effluent outlets. The study provides a novel, integrated assessment framework that links geochemical patterns with ecological risk interpretation, offering baseline data for evidence-based coastal management in the Arabian Gulf. These findings underscore the importance of continuous, multi-seasonal monitoring and biological effect studies to evaluate the long-term ecological implications and inform sustainable industrial and marine spatial planning.

1. Introduction

The Arabian Gulf, one of the world's most industrialized semi-enclosed marine systems, is particularly vulnerable to anthropogenic contamination due to its restricted circulation, high evaporation rates, and shallow water depths. Rapid coastal development, petrochemical industries, desalination plants, and expanding maritime activities have significantly altered the Gulf's sedimentary and ecological environment. Heavy metals (HMs) and metalloids such as Cd, As, Pb, Cu, and Ni are of particular concern because they are persistent, bioaccumulative, and toxic even at low concentrations. Sediments play a dual role as both sinks and secondary sources of these contaminants, influencing benthic habitats and water quality.

Previous studies in the Arabian Gulf have reported variable contamination patterns depending on proximity to industrial and urban discharges (Naser, 2013; Elgendy *et al.*, 2024). However, most investigations have focused on nearshore or estuarine sediments and have rarely incorporated a comprehensive spatial framework linking offshore, midshore, and inshore zones. Moreover, several assessments have relied on single indices or descriptive statistics, without integrating contamination indices with ecological risk evaluations or multivariate

source apportionment. Consequently, there remains a limited understanding of how gradients of industrialization and hydrodynamic conditions influence the spatial distribution and ecological implications of sediment-bound metals and metalloids in the eastern Arabian Gulf.

To address these gaps, this study systematically evaluates the concentration, contamination status, and ecological risks of metals and metalloids in surface seabed sediments collected from 32 locations across the offshore-midshore-inshore continuum of the Arabian Gulf, eastern Saudi Arabia. Jubail represents one of the largest industrial hubs in the Middle East, hosting petrochemical complexes, oil refineries, shipping terminals, and desalination facilities that collectively contribute to multiple pathways of contamination. The study employs a suite of internationally recognized geochemical indices, including the Contamination Factor (CF), Enrichment Factor (EF), Geoaccumulation Index (Igeo), and Potential Ecological Risk Index (PERI), to quantify the intensity of contamination and ecological risk.

Unlike earlier Gulf-based studies that primarily examined overall metal levels, this work integrates multi-index pollution assessment with spatial differentiation among industrially influenced and reference sites, thereby offering a more nuanced understanding of contamination dynamics. Furthermore, Principal Component Analysis (PCA) is

***Corresponding author:**

E-mail address: halfaifi@kacst.gov.sa (H Alfaifi)

Received: 28 August, 2025 Accepted: 09 November, 2025 Epub Ahead of Print: 16 February, 2026 Published: 24 February, 2026

DOI: 10.25259/JKSUS_1366_2025

employed to distinguish between lithogenic and anthropogenic sources, thereby strengthening the interpretation of pollution processes in a complex industrial setting.

By combining contamination metrics, ecological risk indices, and multivariate source analysis, this study provides a robust and spatially explicit assessment of sediment quality in the Jubail coastal zone. The findings contribute new insights into the spatial variability of metal and metalloids contamination, identify cadmium (Cd) and arsenic (As) as priority pollutants, and establish a scientific baseline for sustainable sediment management and regulatory monitoring within the Arabian Gulf.

The present study provides the first integrated, multiscale assessment of HM concentration in Jubail’s coastal sediments, combining high-resolution field sampling, textural analysis, and advanced multivariate statistics to delineate both natural and anthropogenic sources. Unlike Swetha et al. (2025), who performed a meta-analysis of previously published datasets across the Arabian Gulf, this research is based on newly collected sediment samples (2023) that were analyzed for 17 metals using standardized inductively coupled plasma-mass spectrometry (ICP–MS) protocols with rigorous quality control. Furthermore, our study introduces a granulometric dimension, linking sediment composition (sand, silt, and clay fractions) to the potential for metal accumulation, a critical but previously unquantified factor in Gulf sediment studies. This approach enables a mechanistic interpretation of contamination behavior, rather than merely descriptive trends.

Additionally, by employing complementary pollution indices (CF, EF, Igeo, PLI) alongside the PERI and international Sediment Quality Guidelines (SQGs) (threshold effect level (TEL), probable effect levels (PEL), probable effect concentrations (PEC), the study provides a risk-based ecological framework that directly assesses the potential biological consequences of contamination. This level of ecological interpretation was absent in earlier Gulf-wide reviews and regional surveys, such as those by Amin & Almahasheer (2022), which reported general contamination patterns without detailed risk quantification or sediment–metal interaction modelling.

The use of PCA and Cluster Analysis (CA) distinguishes lithogenic metals (Fe, Mn, Ni, Co, Cr) from anthropogenic metals (As, Cd, Cu, Pb, Zn, Ag), revealing spatially confined industrial fingerprints associated with petrochemical effluents, desalination brine discharges, and port activities. This fine-scale diagnostic capability provides actionable insights for targeted mitigation, particularly in Jubail’s nearshore zones, where heavy industrial activity poses ongoing ecological risks.

2. Materials and Methods

2.1 Study area

This study was conducted across offshore, midshore, and inshore zones around Jubail City on the eastern coast of Saudi Arabia (Fig. 1). The region is heavily industrialized, hosting petrochemical complexes, desalination plants, shipping ports, and oil refineries. Given the semi-enclosed nature of the Arabian Gulf, limited water circulation, and high evaporation rates, the area is particularly prone to localized HM enrichment and sediment pollution. To capture spatial variability, 32 surface-seabed sediment samples were collected in December 2023 from strategically selected locations that reflected varying levels of industrial influence, including sites near discharge points, shipping lanes, desalination outfalls, and comparatively pristine offshore reference sites (Fig. 1). Sampling coordinates were recorded using differential GPS for precise spatial mapping.

2.2 Sediment sampling

Sediments were collected using a Van Veen grab sampler and a stainless-steel box corer, both of which are commonly employed in marine sediment studies for minimally disturbed sample retrieval. Each deployment aimed to recover sediments from the upper 0–30 cm of the seabed, the layer most reactive in metal binding. Samples compromised by coarse gravel closure were discarded and re-collected to preserve representativeness. Immediately after collection, sediments were transferred into acid-washed polyethylene containers using plastic

spatulas to minimize contamination, labelled by texture and color, and kept at $-4\text{ }^{\circ}\text{C}$ onboard until lab transport. After each deployment, sampling gear was rinsed with seawater and acid-cleaned to prevent cross-sample contamination.

2.3 Lab preparation and chemical analysis

Sample preparation followed the US EPA/CE-81-1 guidelines for marine sediments. Samples were air-dried for 72 h, gently disaggregated, and passed through a $63\text{ }\mu\text{m}$ sieve to isolate the fine fraction (Que et al., 2024). Fine sediments were stored in acid-cleaned polypropylene vials prior to digestion. Approximately 0.15 g of homogenized sample was weighed into Teflon microwave vessels and digested with a mixture of HNO_3 , HCl, and HF at $170\text{ }^{\circ}\text{C}$ for 50 min, followed by a 30 min hold, using a Milestone ETHOS UP microwave system. Digests were cooled, neutralized with boric acid, and diluted to 50 mL with ultrapure water. Metal quantification was done via ICP-MS (NexION 300D, PerkinElmer, USA) at KACST–NTI. Analysis included major (Fe, Mn, Sr, Ti) and trace metals (Cr, Co, Ni, Cu, Zn, As, Se, Mo, Ag, Cd, Pb, Hf, Sn). Calibration used certified multi-element standards and reference material SRM 2702 – Inorganics in Marine Sediment, with blanks, duplicates (10%), and spike recoveries in every batch. Precision was kept within $\pm 5\%$, recoveries ranged 90% to 105%, and method detection limits ranged from 0.01 to 0.05 mg/kg.

2.4 Sediment texture characterization

The relationship between sediment grain size and metal adsorption was investigated by measuring the sand, silt, and clay fractions using a laser diffraction instrument (Malvern Mastersizer 3000). Pretreatment included the use of hydrogen peroxide to remove organic matter and sodium hexametaphosphate as a dispersant. Sediments were classified according to ASTM D2487 standards. Studies have highlighted that fine particles often carry elevated metal concentrations due to their higher surface area and reactive phases (Que et al., 2024).

2.5 Pollution indices and risk assessment

To evaluate contamination and ecological risk, the following indices were calculated:

- CF: assessed the degree of individual metal enrichment relative to background values (Hakanson, 1980) as follows;

$$CF = \frac{C_i}{C_{b,i}} \dots \dots \dots \quad (1)$$

- EF: normalized metal concentrations against Fe, used as a conservative lithogenic reference (Sutherland, 2000), using this equation.

$$EF = \frac{M_i}{M_{Fe}} \times \frac{C_{Fe}}{C_i} \dots \dots \dots \quad (2)$$

- Geo-accumulation Index (Igeo): classified contamination levels following Müller (1969).

$$I_{geo} = \log_2 \left(\frac{C_n}{1.5 \times B_n} \right) \dots \dots \dots \quad (3)$$

- Pollution Load Index (PLI): provided an integrated measure of overall site contamination (Tomlinson et al., 1980) through Eq. (4).

$$PLI = \sqrt[n]{CF_1 \times CF_2 \times CF_3 \times CF_4 \times \dots \times CF_n} \dots \dots \dots \quad (4)$$

- PERI: estimated ecological risk intensity following Hakanson’s (1980) framework.

$$PERI = \sum_{i=1}^n E_i \dots \dots \dots \quad (5)$$

where

$$E_i = T_i^i \times CF^i \quad (6)$$

Then

$$PERI = \sum_{i=1}^n [T_i^i \times CF^i] \quad (7)$$

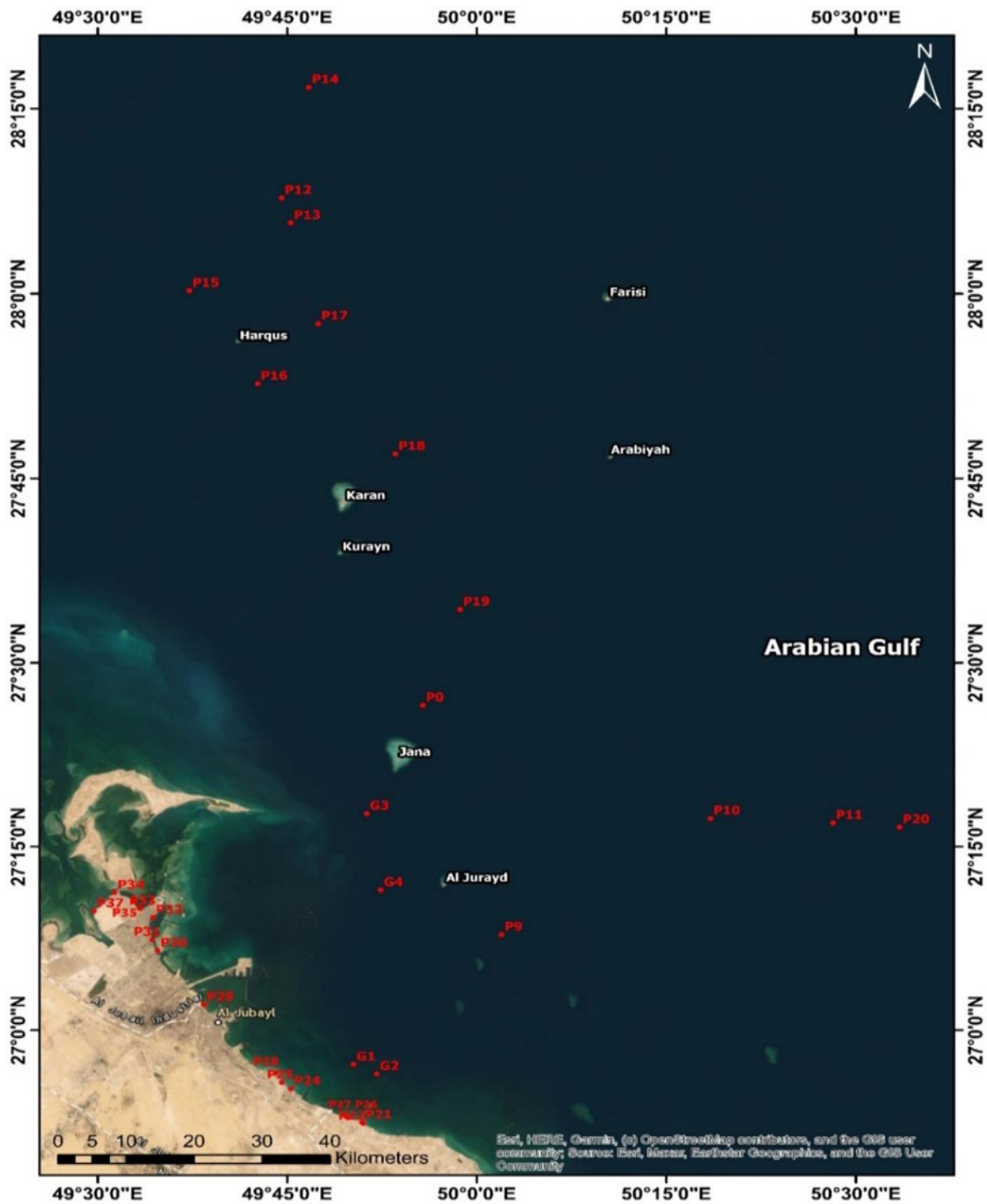


Fig. 1. The location map of the study area shows inshore, midshore, and offshore sampling sites along the Jubail coast in the Arabian Gulf.

We used global average shale values (Turekian & Wedepohl, 1961) and regional baselines for the Arabian Gulf (Naser, 2013) as background references. Recent studies continue to apply this multiparameter framework (Faisal et al., 2025; Salah-Tantawy et al., 2025) to assess HM contamination in sediments and validate source apportionment. Furthermore, to assess ecological risks, sediment metal concentrations were compared against internationally recognized SQGs, including TELs, PELs, and PECs (MacDonald et al., 2000).

The symbols applied in this study are defined as follows: M and C_o denote the analyzed metals, whereas X and C_b represent the levels of the normalizer element. Iron (Fe) was employed as the normalizing element owing to its high abundance in the Earth's crust and its

relatively low mobility under most natural conditions compared with other trace elements. Consequently, Fe provides a reliable reference for assessing natural background levels of metals. C_n refers to the measured concentration of HMs in soils, while B_n indicates the geochemical background concentration of HMs in shale (Taylor and McLennan, 1995). A correction constant of 1.5 was introduced in the calculations to minimize the influence of natural variability in background concentrations (Hakanson, 1980).

The ecological risk associated with metal contamination was further evaluated using a suite of indices. The potential ecological risk factor (E_i^p) quantifies the risk posed by metal i in the sediment (Hakanson, 1980). The toxic-response factor (T_r) reflects both the intrinsic toxicity

of the metal and its relative sensitivity in the environment (Zhang et al., 2016). The CF_i, as defined above, was incorporated into the ecological risk assessment to provide a quantitative measure of metal enrichment. Collectively, these indices enable a comprehensive evaluation of both contamination intensity and its associated ecological consequences (Hakanson, 1980; Cai et al., 2019).

Sediment quality was further interpreted in relation to widely applied SQGs. The TEL is the concentration below which adverse biological effects are unlikely to occur. In contrast, the PEL represents concentrations above which adverse effects are expected to occur more frequently. The PEC denotes concentrations above which adverse effects are highly probable (MacDonald et al., 2000). These benchmarks provide a consistent framework for assessing ecological risks across different environments (Long et al., 1995; MacDonald et al., 2000). The classification schemes and reference values of the indices described above are summarized in Tables 1(a-d), which serve as the basis for evaluating the degree of contamination and potential ecological risk (Hakanson, 1980; Tomlinson et al., 1980; MacDonald et al., 2000).

Statistical analyses were also conducted to interpret spatial patterns, examine relationships among metals, and identify potential sources of contamination. Descriptive statistics, including mean, standard deviation, and coefficient of variation, were calculated for all metals. Pearson correlation analysis was used to evaluate relationships between metals and sediment fractions, indicating possible shared sources. PCA helped differentiate between lithogenic and anthropogenic inputs, while Cluster Analysis (CA) grouped sampling sites based on their similarities in contamination. All statistical analyses were performed using IBM SPSS v26.

PCA was performed using a varimax rotation with Kaiser normalization to maximize the variance explained by each factor and to facilitate clearer interpretation of variable groupings. Components with eigenvalues greater than 1.0 were retained according to the Kaiser

Table 1a. Sediment Quality Guidelines for Metals based on MacDonald et al. (2000) (All values in mg/kg dry weight).

Metal	TEL (threshold effect level)	PEL (probable effect level)	PEC (probable effect concentration)
As (Arsenic)	7.24	41.6	33.0
Cd (Cadmium)	0.676	4.21	4.98
Cr (Chromium)	52.3	160	111
Cu (Copper)	18.7	108	149
Pb (Lead)	30.2	112	128
Hg (Mercury)	0.130	0.696	1.06
Ni (Nickel)	15.9	42.8	48.6
Zn (Zinc)	124	271	459

Table 1b. Contamination Factor (CF) Classification (Hakanson, 1980).

CF Range	Risk Level
CF < 1	Low
1 ≤ CF < 3	Moderate
3 ≤ CF < 6	Considerable
CF ≥ 6	Very High

Table 1c. Enrichment Factor (EF) Classification (Sutherland, 2000).

EF Range	Risk Level / Source Inference
EF < 2	Minimal / Natural source
2 ≤ EF < 5	Moderate / Possible anthropogenic
5 ≤ EF < 20	Significant / Anthropogenic
20 ≤ EF < 40	Very High / Strong anthropogenic
EF ≥ 40	Extremely High / Extreme enrichment

Table 1d. Geoaccumulation Index (Igeo) Classification (Müller, 1969).

Igeo Range	Pollution Intensity
Igeo ≤ 0	Unpolluted
0 < Igeo ≤ 1	Unpolluted to moderately polluted
1 < Igeo ≤ 2	Moderately polluted
2 < Igeo ≤ 3	Moderately to heavily polluted
3 < Igeo ≤ 4	Heavily polluted
4 < Igeo ≤ 5	Heavily to extremely polluted
Igeo > 5	Extremely polluted

criterion, and only factor loadings ≥ 0.6 were considered significant in defining the association between metals and principal components. These criteria ensured that the extracted components captured the dominant geochemical patterns with minimal redundancy and improved interpretability.

3. Results and Discussion

3.1 Sediment texture and granulometry

The sediments from offshore and inshore sampling sites were predominantly sandy-silt with minor clay fractions. Grain size analysis revealed that offshore sites were dominated by sand (65–80%), whereas inshore sediments closer to industrial discharge zones contained higher proportions of silt and clay (30–45%) (Tables 2a and b). Poorly graded sands characterized coastal sites, whereas offshore sediments exhibited higher silt and clay content, especially near South Jana and North Karan Islands. This spatial distribution is typical of semi-enclosed marine systems (Fig. 2), where fine particles tend to settle in sheltered areas with lower hydrodynamic energy (ASTM D2487, 2011). Fine-grained sediments are known to have higher metal adsorption capacity due to larger specific surface area and higher organic matter content (Forstner & Wittmann, 2012; He et al., 2020).

3.2 Heavy metal concentrations

Table 3 summarizes the average, minimum, and maximum concentrations of major and trace metals across all sampling sites. HM concentrations varied across the study area. Iron (Fe) was the most abundant metal (mean: 5163 mg/kg), followed by manganese (Mn: 148 mg/kg) and chromium (Cr: 82 mg/kg). Potentially toxic metals such as arsenic (As: 24.8 mg/kg), lead (Pb: 4.8 mg/kg), and cadmium (Cd ≤ 2.4 mg/kg) mainly were below National Oceanic and Atmospheric Administration, NOAA, PECs, although localized exceedances of As, Ag, Cd, and Co were detected at sites P9, P11, P14, and P29. Notably, As exceeded 33 mg/kg PEC in five sites, suggesting moderate ecological concern (Long et al., 1995). Elevated Zn and Cu were found inshore, reflecting inputs from industrial effluents and urban runoff, while Fe, Mn, Ni, and Co primarily reflected lithogenic contributions from natural sediment sources. Spatial distributions of lithogenic and anthropogenic metals are illustrated in Figs. 3 and 4. Moreover, Fig. 5 shows the boxplots of key metals (As, Cd, Pb, Zn, Cu), highlighting variability across sites and potential exceedances. Notably, As and Cd displayed greater variability and occasional elevations, whereas Pb and Zn remained low and stable. This pattern reflects localized anthropogenic input over a background of predominantly lithogenic metals.

3.3 Spatial variations and site-based ranking of metal contamination

To better integrate site-specific variations, metal contamination levels across the 32 sampling sites were compared using CFs and the PLI. The calculated CFs for ten metals (Cr, Mn, Fe, Co, Ni, Cu, Zn, As, Cd, Pb) and corresponding PLI values have been presented in Table 4. PLI values ranged from 0.12 to 0.80, indicating generally low to moderate contamination across the study area.

The highest contamination was observed at Sites P11, P14, P13, P12, and P16, with PLI values ranging from 0.64 to 0.80, suggesting

Table 2a.
Sediment classifications of inshore, midshore, and offshore sampling survey.

Site ID	Location/description	Latitude	Longitude	Color	Sand %	Silt%	Clay%	Gravel%	Sieve Analysis ASTM D 2487 Soil Classification
G1	Open sea, Jubail	26°57'11.81"N	49°50'14.10"E	Gray	89.5	9.5	0.2	0.8	Poorly Graded Sand with Silt
G2	Open sea, Jubail	26°56'25.30"N	49°52'5.02"E	Brown	96.5	0.7	2.8	0	Well-graded Sand
G3	Open sea, South JANA Island on Seismic line	27°17'42.65"N	49°51'17.17"E	Gray	40.5	58.5	1	0	Sandy Lean Clay
G4	Open sea, AL JURAID Island (West)	27°11'27.71"N	49°52'24.06"E	White	97.6	1.9	0	0.5	Poorly Graded Sand
P0	Open sea, South JANA Island	27°26'31.75"N	49°55'43.76"E	Gray	NA	NA	NA	NA	NA
P9	Open sea, South JANA Island	27° 7'49.17"N	50° 1'57.13"E	Gray	26	72.8	1.2	0	Lean Clay with Sand
P10	Open sea, South JANA Island	27°17'18.73"N	50°18'29.07"E	Gray	78.2	21.3	0.4	0.1	Silty Sand
P11	Open sea, South JANA Island	27°16'57.03"N	50°28'11.02"E	Gray	15.8	82.8	1.4	0	Silt with Sand
P12	Open sea, North KARAN Island	28° 7'46.03"N	49°44'33.42"E	Gray	40.5	58.4	1	0.1	Sandy Lean Clay
P13	Open sea, North KARAN Island	28° 5'44.59"N	49°45'16.39"E	Gray	50.7	48.5	0.8	0	Silty Sand
P14	Open sea, North KARAN Island	28°16'43.92"N	49°46'42.53"E	Gray	51.2	48	0.8	0	Silty Sand
P15	Open sea, North KARAN Island	28° 0'15.30"N	49°37'15.20"E	Gray	58.5	40.8	0.7	0	Silty Sand
P16	Open sea, North KARAN Island	27°52'42.30"N	49°42'39.67"E	Gray	31.9	67	1.1	0	Sandy Silt
P17	Open sea, North KARAN Island	27°57'34.22"N	49°47'26.90"E	Gray	30.8	68	1.2	0	Sandy Silt
P18	Open sea, North KARAN Island	27°46'59.99"N	49°53'33.38"E	Gray	40.1	58.7	1	0.2	Sandy Silt
P19	Open sea, South KARAN Island	27°34'20.47"N	49°58'40.16"E	Gray	31	67.8	1.2	0	Sandy Silt
P20	Open sea, South KARAN Island	26°52'32.00"N	49°50'48.10"E	Gray	20.7	77.9	1.4	0	Lean Clay with Sand
P21	Coastal, Ras Al Ghar	26°52'26.30"N	49°50'55.90"E	White	99.1	0.3	0	0.6	Poorly Graded Sand
P22	Coastal, Ras Al Ghar	26°52'21.40"N	49°51'0.20"E	White	99.1	0.5	0	0.4	Poorly Graded Sand
P24	Coastal, Jubail	26°55'11.94"N	49°45'16.59"E	White	96.6	0.5	0	2.9	Poorly Graded Sand
P25	Coastal, Jubail	26°55'43.20"N	49°44'34.00"E	White	95	0.8	0	4.2	Poorly Graded Sand
P26	Coastal, Ras Al Ghar	26°52'50.70"N	49°49'48.20"E	White	98.7	1	0	0.3	Poorly Graded Sand
P27	Coastal, Ras Al Ghar	26°52'57.25"N	49°49'38.30"E	White	99.9	0.1	0	0	Poorly Graded Sand
P28	Costal, Jubail	26°56'28.63"N	49°44'4.10"E	White	90.5	0.6	0	8.9	Poorly Graded Sand
P29	Coastal, Jubail City Center	27° 2'5.48"N	49°38'24.10"E	Brown	95.9	0.3	0	3.8	Poorly Graded Sand
P30	Coastal, Jubail	27° 6'31.05"N	49°34'44.65"E	Brown	98.8	1.2	0	0	Poorly Graded Sand
P31	Coastal, Jubail	27° 7'23.72"N	49°34'18.60"E	Gray	92.5	0.4	0	7.1	Poorly Graded Sand
P32	Coastal, Jubail	27° 9'12.64"N	49°34'21.77"E	Brown	98.1	0.1	0	1.8	Poorly Graded Sand
P33	Coastal, Jubail	27° 9'56.83"N	49°33'19.99"E	Brown	97.7	1	0	1.3	Poorly Graded Sand
P34	Coastal, Jubail	27°11'14.81"N	49°31'19.96"E	Brown	98.2	0.7	0	1.1	Poorly Graded Sand
P35	Coastal, Jubail	27°10'29.68"N	49°32'54.96"E	Brown	97.4	0.6	0	2	Poorly Graded Sand
P37	Coastal, Jubail	27° 9'44.61"N	49°29'42.06"E	Brown	99.5	0.3	0	0.2	Poorly Graded Sand

Table 2b.
Sediment Grain Size Distribution. Grain size distribution in offshore, midshore, and inshore sediments along the Jubail coastal zone. Inshore sediments have higher silt and clay fractions, which increase their capacity to retain heavy metals compared to coarser offshore sediments.

Site group	Sand (%)	Silt (%)	Clay (%)	Texture class
Offshore (n=12)	65–80	15–25	5–10	Sandy silt
Midshore (n=10)	50–65	25–35	10–15	Silty sand
Inshore (n=10)	40–55	30–40	15–20	Sandy clay silt

localized enrichment likely influenced by anthropogenic sources, such as port operations and effluent discharge. The most dominant contaminants at these sites were As, Co, and Ni, which exhibited CF values exceeding 1.0, indicating moderate contamination levels. In contrast, the lowest PLI values (≤ 0.20) were recorded at Sites P28, P24, P20, and P35, reflecting background or near-natural conditions.

Spatially, contamination followed a declining gradient from the inner harbor and industrially influenced zones toward the open marine stations, suggesting dilution and sediment mixing effects. The ranking clearly delineates potential contamination hotspots and supports prioritization for ecological risk evaluation and management.

To further differentiate site contamination levels, the measured metal concentrations were compared with the US EPA mean baseline levels for uncontaminated soils (EPA, 2015; ATSDR, 2022). Sites P11–P16 surpassed the baselines for As, Co, and Ni, confirming localized anthropogenic enrichment, while most offshore sites remained below the EPA thresholds

3.4 Spatial heterogeneity and dominant metal patterns

The integration of site-specific contamination indices reveals distinct spatial patterns in HM distribution, providing new insights beyond the overall concentration trends discussed earlier (Table 4). Sites such as P11–P16, located closer to industrial outfalls and navigation channels, consistently showed elevated CFs for As, Co, and Ni, reflecting contributions from metallurgical effluents and ship maintenance activities. Arsenic dominance in several sites (e.g., P11, P13) suggests possible inputs from fuel combustion and antifouling paints, aligning with patterns reported in other coastal sediment studies (Swarnakar et al., 2024).

Moderate enrichment in Co and Ni at the mid-channel sites may also be associated with hydrodynamic trapping and organic matter binding, as these metals often exhibit particle-reactive behavior. The low-PLI sites, particularly P28–P24, exhibited metal levels close to geochemical

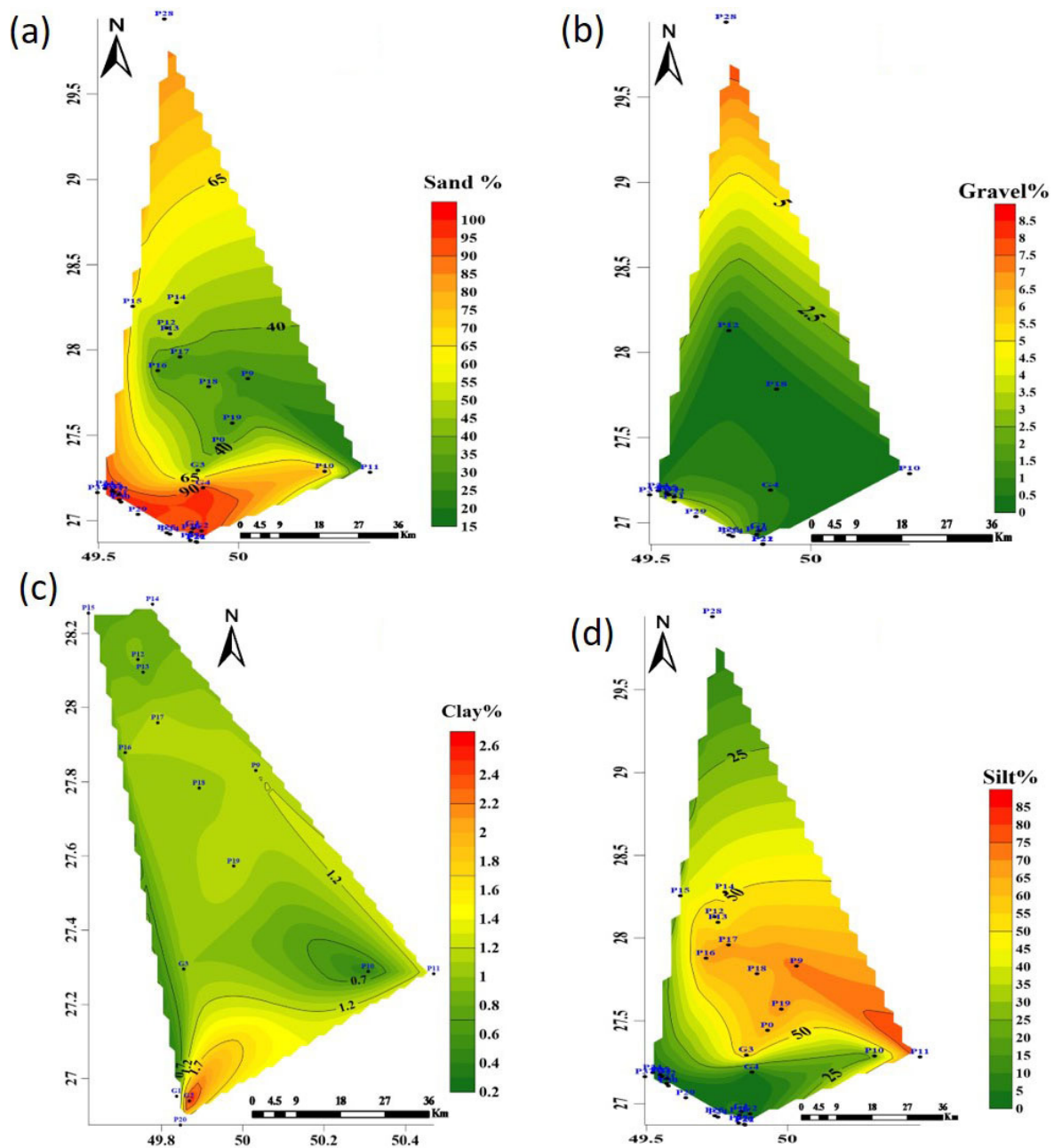


Fig. 2. Grain size distribution of surface seabed sediments at different site groups illustrates higher silt and clay fractions nearshore. Four soil classifications of (a) sand, (b) gravel, (c) clay, and (d) silt were plotted as given in Table 2a.

background values, confirming the limited anthropogenic influence in offshore areas. By ranking sites and identifying dominant metals, this analysis provides a spatially explicit framework for evaluating the intensity of contamination and its ecological implications. Such an approach strengthens sediment quality assessment by pinpointing priority zones for monitoring and remediation.

The classification of sites using US-EPA mean soil baseline values supports the PLI-based ranking and reinforces the identification of As-, Co-, and Ni-dominated hotspots. The agreement between these two independent approaches underscores the robustness of the spatial assessment framework.

3.5 Integrated contamination, source apportionment, and ecological risk implications

To comprehensively assess the contamination status and ecological implications of HMs in Jubail coastal sediments, multiple indices, including the CF, EF, Geoaccumulation Index (Igeo), PLI, and PERI,

were integrated with multivariate statistical analyses (Tables 5-8; Figs. 6-8).

Across all sites, most metals (Cr, Ni, Cu, Pb, Co, Mn, Fe) exhibited $CF < 1$ and low Igeo values, confirming their primarily lithogenic origin with minimal anthropogenic enrichment. In contrast, cadmium (Cd) and arsenic (As) were distinctly elevated, with CF values of 5.03 and 1.82 and EFs of 46.01 and 2.36, respectively. The levels of EF for Cd indicate anthropogenic inputs, likely linked to petrochemical effluents, desalination brine discharges, and port-related activities. In contrast, the enrichment of As is attributed to antifouling coatings, fuel combustion, and industrial runoff.

The PLI values ranged from 0.48 to 0.85 across all sampling zones, remaining below the pollution threshold ($PLI = 1.0$), which classified the sediments as generally unpolluted (Tomlinson et al., 1980). However, inshore areas recorded higher PLI values (0.85), reflecting localized industrial influence and reduced hydrodynamic dispersion. This spatial gradient was reflected in the PERI results, with inshore sediments showing moderate ecological risk ($PERI = 225.7$), midshore

Table 3. HM Concentrations in Surface Sediments (mg/kg). *Background values from world average shale (Turekian & Wedepohl, 1961); TEL/PEL from MacDonal et al. (2000). Summary of HM concentrations in surface sediments from the Jubail coast. Arsenic (As) exceeds the PEL at some inshore sites, indicating localized ecological risk. Other metals remain below guideline thresholds.

Metal	Max.	Min.	Mean ± SD	Background (mg/kg)	TEL (mg/kg)	PEL (mg/kg)
Cr	232	8.76	82.2 ±12.45	90	52.3	160
Mn	452	9.33	148.3 ±25.34	850	N/A	N/A
Fe	20900	355	5163 ±1010.38	47200	N/A	N/A
Co	54.3	3.24	16.3 ±1.95	19	N/A	N/A
Ni	105	8.72	33.2 ±4.94	68	15.9	42.8
Cu	137	1.64	26.6 ±4.84	45	18.7	108
Zn	83	1.44	20.0 ±3.36	95	124	271
As	65.3	2.9	24.8 ±3.15	13	7.24	41.6
Sr	3720	272	1810.8 ±163.91	350	N/A	N/A
Mo	1.01	0.13	0.4 ±0.04	2.6	N/A	N/A
Ag	1.99	0.23	0.9 ±0.08	0.07	N/A	N/A
Cd	2.42	0.03	0.6 ± 0.3	0.3	0.676	4.21
Pb	23.9	1.01	4.78 ± 0.74	20	30.2	112
Hf	1.06	0.06	0.39 ± 0.092	3	N/A	N/A
Sn	3.9	0.16	0.87 ±0.13	2.5	N/A	N/A
Ti	1260	68.1	60.34 ±455	4400	N/A	N/A

sediments indicating low risk (PERI = 138.2), and offshore sediments indicating minimal risk (PERI = 93.6). Cadmium contributed a total ecological risk (ER_i = 151), while As contributed moderately (ER_i = 18.2). The remaining metals exhibited ER_i < 40, confirming that localized enrichment of Cd and As drives the ecological risk in this system.

Statistical correlations and source apportionment analyses (Pearson's correlation and PCA) revealed two distinct metal groupings. The PCA model retained two principal components with eigenvalues > 1.0, cumulatively explaining 78.4% of the total variance. The use of varimax rotation with Kaiser normalization improved interpretability, distinguishing a lithogenic component (Fe, Mn, Cr, Ni, Co) from an anthropogenic component (Cd, As, Cu, Zn, Pb). High loadings of Cd and As on the second component, combined with elevated PERI scores in inshore sediments, confirm that industrial and port activities are the primary sources of contamination. These results closely correspond to patterns observed in other Gulf coastal zones, such as Abu Ali Island, where Cd and As similarly dominate anthropogenic signatures (Mahboob et al., 2022).

Ecological and spatial implications derived from the PERI and PCA analyses indicate that although overall contamination levels remain low to moderate, hotspots of Cd and As enrichment near industrial discharge zones present clear ecological concern. These elements are highly mobile and bioavailable in fine-grained sediments, increasing their potential to accumulate in benthic invertebrates such as polychaetes, bivalves, and crustaceans (Mohamed et al., 2024). Continuous sediment resuspension and particle ingestion enhance metal bioaccumulation, facilitating trophic transfer to demersal fish and filter-feeding organisms.

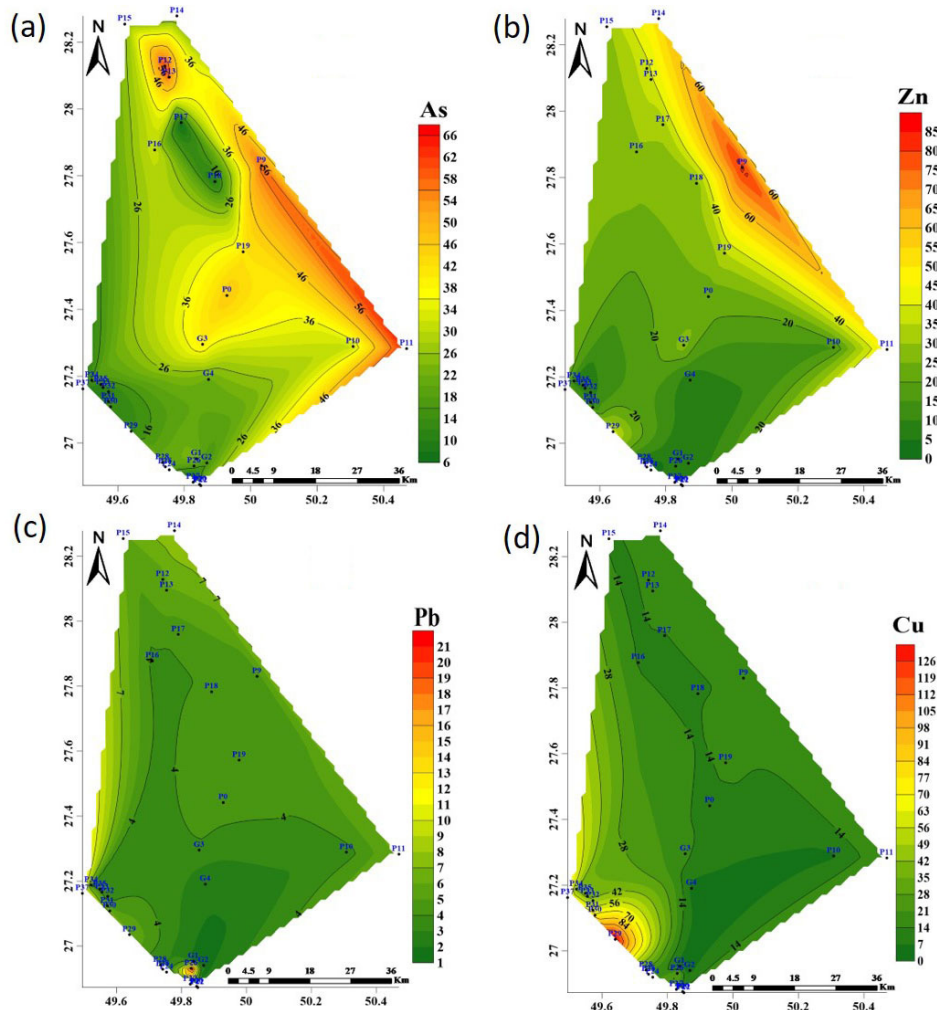


Fig. 3. Spatial distribution maps of lithogenic metal concentrations, for (a) As, (b) Zn, (c) Pb, and (d) Cu, in surface sediments demonstrate localized hotspots near industrial zones.

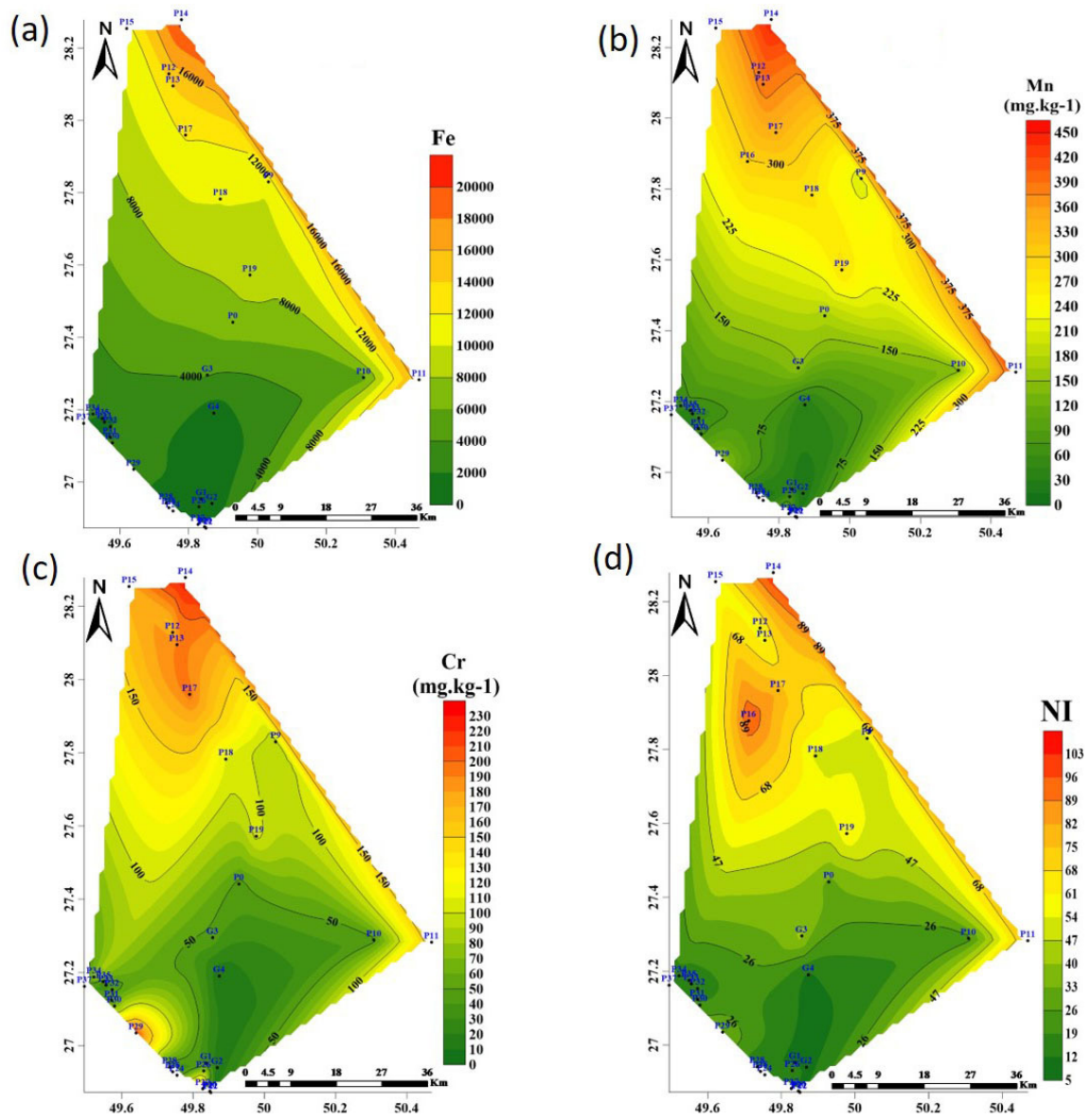


Fig. 4. Spatial distribution maps of anthropogenic metal concentrations for (a) Fe, (b) Mn, (c) Cr, and (d) Ni, in surface sediments display localized hotspots near industrial zones.

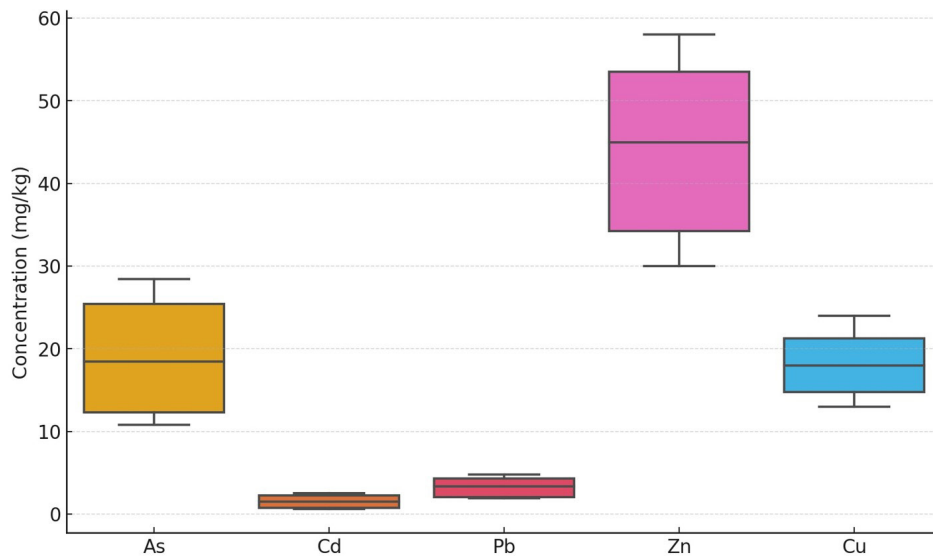


Fig. 5. Boxplots of key metals As, Cd, Pb, Zn, and Cu show variability and potential exceedances.

Table 4.
Ranking of sampling sites by total contamination (PLI) and by individual HMs

Site	PLI	Rank	CF_Mn	CF_Fe	CF_Co	CF_Ni	CF_Cu	CF_Zn	CF_As	CF_Pb	Dominant contaminant
P11	0.80	1	0.51	0.37	1.64	1.16	0.47	0.52	5.02	0.32	As, Co, Ni
P14	0.76	2	0.53	0.44	1.42	1.54	0.44	0.57	1.67	0.41	As, Co, Ni
P13	0.68	3	0.46	0.23	1.421	0.85	0.32	0.41	4.38	0.3	As, Co
P12	0.66	4	0.45	0.31	1.15	0.86	0.33	0.4	4.88	0.28	As, Co
P16	0.65	5	0.35	--	0.96	1.41	0.3	0.31	2.43	0.19	Ni, As
P9	0.63	6	0.25	0.22	1.41	0.74	0.34	0.87	4.44	0.22	Co, As
P15	0.56	7	0.39	0.26	1.55	0.81	0.27	0.31	1.95	0.29	Co, As
P19	0.55	8	0.33	0.19	0.73	0.88	0.38	0.36	3.2	0.25	As
P0	0.48	9	0.2	0.15	2.85	0.45	0.21	0.22	3.55	0.22	Co, As
P17	0.478	10	0.4	0.25	1.2	1.18	0.31	0.33	0.4	0.21	Co, Ni
P29	0.48	11	0.19	0.07	0.45	0.51	3.04	0.42	1	0.31	As
P18	0.44	12	0.32	0.21	1.042	0.76	0.3	0.28	0.64	0.21	Co
G3	0.40	13	0.18	0.09	0.39	0.63	0.38	0.3	3.09	0.19	As
P26	0.33	14	0.08	0.04	0.52	0.29	0.71	0.09	1.36	1.2	As, Pb
P10	0.32	15	0.16	0.11	0.71	0.33	0.13	0.15	2.43	0.17	As
P37	0.28	16	0.04	0.04	0.17	0.21	1.68	0.25	0.74	0.65	Cu
P30	0.28	17	0.06	0.05	0.26	0.29	1.54	0.07	1.03	0.29	Cu, As
P34	0.26	18	0.08	0.05	0.43	0.21	0.87	0.06	1.4	0.17	As
P31	0.25	19	0.04	0.03	0.43	0.28	1.42	0.09	0.7	0.23	Cu
P25	0.23	20	0.067	0.03	0.61	0.19	0.42	0.05	3.12	0.11	As
P32	0.22	21	0.06	0.05	0.17	0.19	1.01	0.09	0.82	0.17	Cu
P27	0.21	22	0.14	0.05	0.32	0.24	0.56	0.09	0.22	0.14	Cu
P33	0.19	23	0.03	0.03	0.29	0.15	0.84	0.07	0.78	0.17	As
G1	0.18	24	0.03	0.03	1.39	0.15	0.08	0.07	1.85	0.09	Co, As
P22	0.18	25	0.02	0.02	0.63	0.15	0.4	0.05	1.82	0.11	As, Co
P35	0.17	26	0.01	0.02	0.23	0.18	0.77	0.064	0.83	0.18	As, Cu, Zn
G4	0.16	27	0.03	0.02	0.71	0.15	0.1	0.057	1.63	0.11	As, Co
P21	0.16	28	0.02	0.02	0.86	0.17	0.32	0.03	0.71	0.11	Co, As
G2	0.15	29	0.02	0.03	1.33	0.14	0.08	0.07	1.18	0.08	Co, As
P28	0.14	30	0.01	0.01	0.94	0.17	0.4	0.02	1.67	0.14	As, Co
P24	0.14	31	0.02	0.01	0.71	0.18	0.43	0.021	1.29	0.06	As, Co
P20	0.12	32	0.03	0.02	0.38	0.13	0.036	0.06	0.67	0.12	As

Table 5.

Mean concentrations of metals and metalloid (As), CFs, geo-accumulation indices (Igeo), EFs, and ecological risk factors (ERI) in surface seabed sediments collected from offshore, midshore, and inshore zones of the Arabian Gulf.

Metal	Mean (mg/kg)	Range (mg/kg)	Background (mg/kg)	CF	Igeo	EF	Risk factor (ERI)	Ecological risk category
Cr	38.5	15.2–91.3	90	0.43	– 0.74	0.85	4.3	Low
Mn	250	180–490	850	0.29	– 1.10	0.62	1.5	Low
Fe	36,200	21,000–47,800	47,200	0.77	– 0.32	—	—	—
Co	17.1	6.3–33.4	19	0.9	– 0.10	1.12	8.9	Low
Ni	45.7	21.8–91.6	68	0.67	– 0.31	1.24	11.3	Low
Cu	27.4	12.6–62.3	45	0.61	– 0.36	1.09	6.1	Low
Zn	115.2	68.1–195.5	95	1.21	0.06	1.65	3.5	Low
As	23.7	9.2–53.4	13	1.82	0.23	2.36	18.2	Moderate
Cd	1.51	0.32–3.94	0.3	5.03	0.94	46.01	151	Very High
Pb	17.6	6.7–38.3	20	0.88	– 0.12	1.21	7	Low
Mean ± SD	—	—	—	1.36 ± 1.49	—	—	23.5 ± 45.7	—

Benthic macrofauna, which is essential for sediment oxygenation and nutrient cycling, may experience sublethal stress under elevated Cadmium exposure ($ER_1 = 151$), potentially leading to biodiversity loss

and altered biogeochemical processes. Similar Cd-linked ecological effects have been reported in other Gulf sediments impacted by industrial effluents and refinery discharges (Naser, 2013). Although

Table 6. Integrated Site Pollution and Ecological Risk. PLI and PERI by site group. Inshore areas near industrial discharge points show localized moderate ecological risks, while offshore sites remain with low risk.

Site group	PLI	PERI	PLI risk	PERI risk
Inshore	0.85	225.70	Unpolluted	Moderate Risk
Midshore	0.62	138.23	Unpolluted	Low Risk
Offshore	0.48	93.57	Unpolluted	Low Risk

Table 7. PCA Loadings for Metal Groupings in Jubail Sediment illustrating how PC1 represents lithogenic sources (natural sediment inputs) and PC2 captures anthropogenic contamination (from industrial, urban, and shipping activities).

Metal	PC1 loading	PC2 loading	Group interpretation
Fe	0.88	0.1	Lithogenic
Mn	0.85	0.12	Lithogenic
Co	0.82	0.18	Lithogenic
Ni	0.79	0.22	Lithogenic
Cr	0.76	0.25	Lithogenic
Ti	0.74	0.28	Lithogenic
As	0.32	0.76	Anthropogenic
Zn	0.27	0.81	Anthropogenic
Cu	0.25	0.83	Anthropogenic
Ag	0.21	0.79	Anthropogenic
Cd	0.18	0.85	Anthropogenic
Pb	0.15	0.82	Anthropogenic

Table 8. Comparison of PLI and PERI across coastal zones.

Zone	PLI	PLI interpretation	PERI	PERI interpretation
Inshore	0.85	Unpolluted	225.7	Moderate risk
Midshore	0.62	Unpolluted	138.2	Low risk
Offshore	0.48	Unpolluted	93.6	Low risk

the integrated PERI values suggest generally low regional risk, the disproportionate contribution of Cd highlights the need for continued biological monitoring using bioassay and biomarker-based approaches to validate theoretical risk indices (Mohamed et al., 2024).

Spatially, elevated PERI scores and anthropogenically influenced PCA loadings co-occurred at sites adjacent to industrial discharges, shipping lanes, and desalination. In contrast, lithogenic elements (Fe, Mn, Cr) associated with natural geogenic processes were strongly loaded onto the secondary component, reflecting background sediment contributions from coastal erosion and resuspension. This spatial correspondence between PCA groupings and ecological risk metrics validates the integrated multi-index approach, which links contamination sources, geochemical behavior, and ecological implications.

Although the PERI and related indices suggest moderate ecological risk in localized zones, they provide a quantitative framework for estimating potential risk, but not actual biological impact. Accordingly, the present findings should be viewed as precautionary indicators of potential ecological stress rather than definitive measures of biological harm. Integrating future bioassay data and benthic community analyses will be critical to confirm the sediment–biota linkages implied by the current geochemical results.

3.6 Unique perspectives and implications for coastal management

The results of this study offer a shift from region-wide descriptive trends to site-specific process understanding. Whereas Swetha et al. (2025) concluded that the Arabian Gulf exhibits low-to-moderate contamination with industrial hotspots, our findings reveal that micro-environmental variations in sediment texture and hydrodynamic energy strongly govern metal enrichment and ecological risk at the sub-kilometer scale. The identification of fine-grained sediment traps near discharge outlets as preferential zones for As and Cd accumulation highlights the mechanistic linkage between sediment dynamics, providing a predictive framework for future coastal management and restoration.

3.7 Temporal scope and baseline nature of the study

This investigation was designed as a spatially explicit baseline assessment of HM contamination in Jubail’s coastal sediments rather

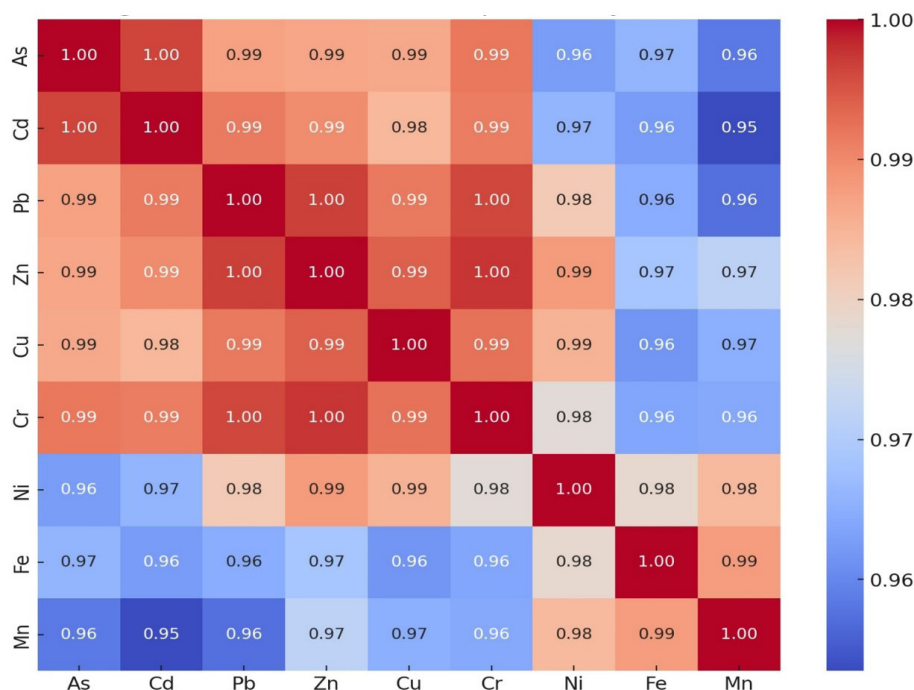


Fig. 6. The correlation heatmap displays the lithogenic vs. anthropogenic grouping of metals.

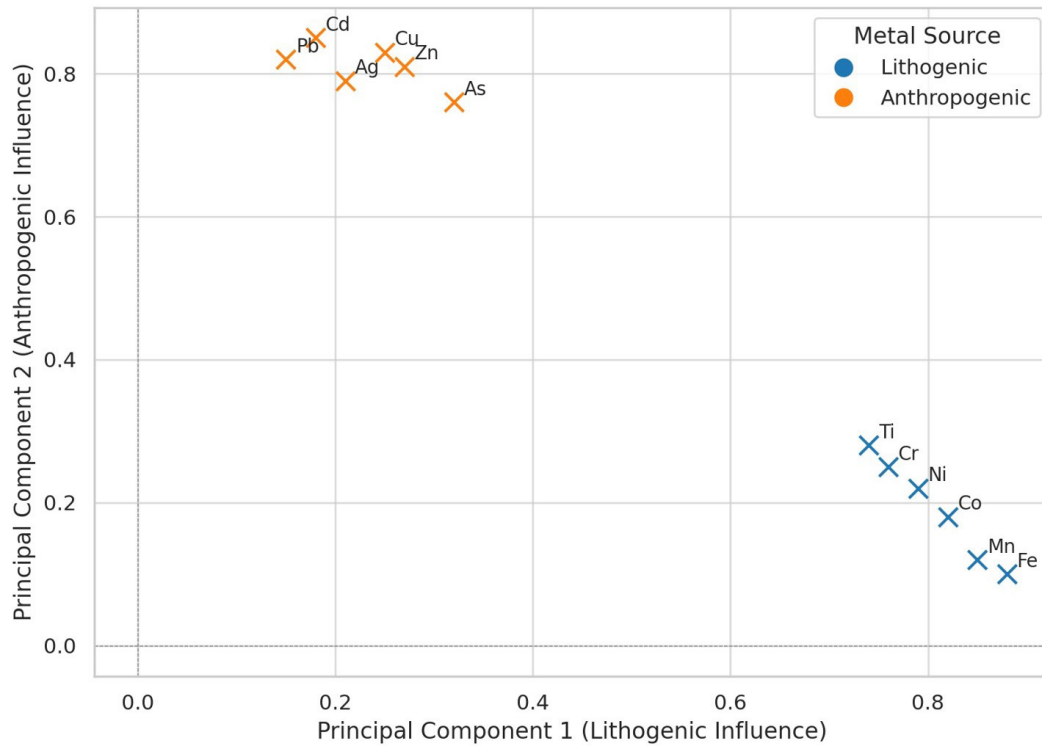


Fig. 7. PCA Biplot for HM source identification indicates natural and anthropogenic metal sources.

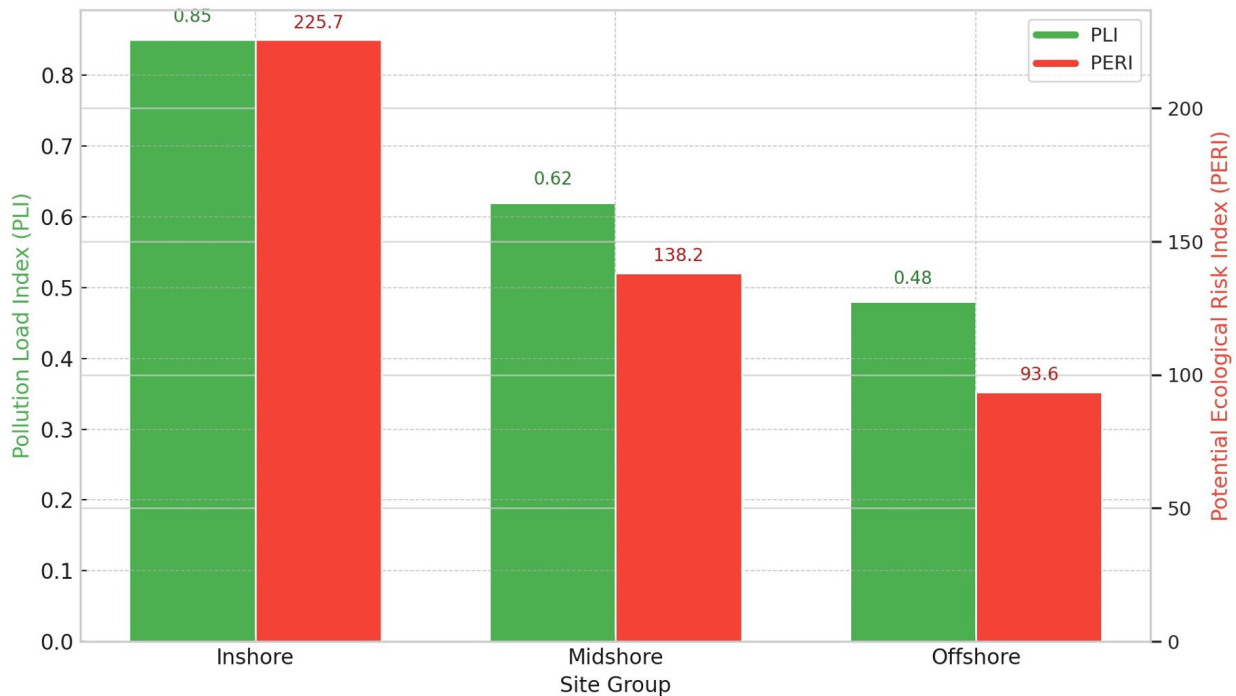


Fig. 8. Comparison of PLI and PERI for inshore, midshore, and offshore sites.

than a temporal monitoring study. The sampling campaign, conducted in December 2023, coincided with hydrographically stable conditions characterized by minimal storm or tidal disturbance. This timing was intentional to minimize short-term variability associated with sediment resuspension and to establish a reliable reference dataset under relatively steady environmental conditions. Although this approach provides a robust spatial characterization of contamination and ecological risk, we acknowledge that metal deposition and bioavailability can

vary seasonally, influenced by fluctuations in hydrodynamic energy, industrial discharge cycles, and variations in runoff intensity. Therefore, while the present findings effectively define baseline contamination patterns, they should be interpreted as representing a snapshot of steady state within the annual cycle. Subsequent multi-seasonal and multi-year monitoring will be valuable for capturing dynamic temporal trends and refining risk assessments under variable environmental conditions.

It is important to note that the current assessment serves as a geochemical baseline rather than a comprehensive ecotoxicological evaluation. While the indices applied (CF, EF, Igeo, PLI, and PERI) provide strong predictive insights into contamination intensity and potential ecological risk, they do not substitute for direct biological testing. No bioassay or organismal data were collected as part of this initial survey, and therefore, the inferred ecological risks should be interpreted as indicative rather than confirmatory. Future investigations will incorporate sediment bioassays and biomarker-based assessments to validate these theoretical risk predictions and enhance understanding of biological exposure pathways within the Jubail coastal ecosystem.

3.8 Management and monitoring implications

In response to the enrichment of cadmium (Cd) and arsenic (As) in inshore sediments and the moderate ecological risk levels observed, several management actions are recommended to mitigate contamination and enhance policy relevance.

- (1) Monitoring intervals: A biannual to annual monitoring schedule (every 6–12 months) is proposed for industrial and near-port sediment zones, with extended intervals (approximately every 24 months) for mid- and offshore areas where contamination indices (PLI < 1.0 and PERI < 150) indicate lower risk. Such periodic monitoring aligns with current regional recommendations for heavy-metal surveillance in coastal ecosystems (Swetha et al., 2025).
- (2) Effluent and discharge control: Given the strong anthropogenic signal of Cd and As linked to petrochemical, desalination, and port operations, implementation of pre-treatment and heavy-metal removal systems (e.g., adsorption, precipitation, or filtration technologies) prior to discharge is recommended. Industrial effluent guidelines should specify concentration limits and require routine reporting. Similar strategies have proven effective in coastal industrial zones worldwide (El-Sharkawy et al., 2025).
- (3) Hotspot remediation: For sites exhibiting “moderate” ecological risk (PERI > 200), targeted mitigation should be prioritized. Sediment capping, dredging, or in-situ stabilization using low-impact materials may reduce contaminant mobility and bioavailability, as supported by sustainable remediation case studies.
- (4) Adaptive management and stakeholder engagement: An adaptive management framework is recommended, whereby updated sediment data guide management decisions in each monitoring cycle. This approach should involve coordination among industry operators, port authorities, environmental agencies, and local stakeholders to enhance transparency and ensure compliance (El-Sharkawy et al., 2025).
- (5) Integration of indices in regulatory frameworks: The PLI and PERI employed in this study could serve as early-warning indicators for sediment quality management. Trigger levels (e.g., PLI > 1.0 or PERI > 300) may be incorporated into environmental monitoring protocols to signal when management actions are required. Similar index-based monitoring systems have been successfully implemented in other Gulf regions (Swetha et al., 2025).

4. Conclusions

This study provides the first integrated, multiscale assessment of HM and metalloid contamination in the seabed sediments of Jubail Industrial City, eastern Saudi Arabia. By coupling geochemical indices (CF, EF, Igeo, PLI, PERI) with multivariate analyses (PCA), it distinguishes between lithogenic background inputs and localized anthropogenic enrichment, providing a mechanistic understanding of sediment contamination processes in one of the Arabian Gulf's most industrialized coastal systems.

From a management perspective, the study underscores the importance of continuous, site-specific monitoring using integrated indices and biological endpoints to track early ecological responses. Future work should focus on multi-seasonal monitoring, biological uptake studies, and ecotoxicological modeling to quantify long-term trends and assess the implications for food webs. Incorporating

biological indicators such as benthic invertebrate diversity, biomarker responses, and fish tissue analyses will bridge the gap between geochemical risk assessment and ecological function.

The study advances regional understanding of sediment-metal dynamics by providing a reproducible, ecologically grounded, and policy-relevant framework for managing coastal sediment quality in the context of ongoing industrial expansion. Its approach and findings have broader applicability to other semi-enclosed marine environments facing similar contamination pressures, supporting evidence-based regulation and sustainable coastal development across the Arabian Gulf and beyond.

CRediT authorship contribution statement

Majed A. Almalki and Hassan Y. Alfaifi wrote the manuscript with input from all authors and supervised the project; **Hany M. Almotairy and Khaled N. Alharbi** conceived and planned the experiments. **Hassan Y. Alfaifi** contributed to the interpretation of the results. **Khaled N. Alharbi and Musaad K. Aleid** contributed to sample preparation and performed the experiments. **Mubarak M. Albarqi and Raed A. Alsulami** contributed to writing and reviewing the results. All authors provided critical feedback, helped shape the research and analysis, and contributed to the final manuscript.

Declaration of competing interest

The authors declare that they have no competing financial interests or personal relationships that could have influenced the work presented in this paper.

Data availability

The data are available upon request from the corresponding author.

Declaration of Generative AI and AI-assisted technologies in the writing process

The authors confirm that there was no use of Artificial Intelligence (AI)-Assisted Technology for assisting in the writing or editing of the manuscript and no images were manipulated using AI.

Acknowledgment

We would like to thank both the scientific research vessel (TAQNIA) for collecting samples from the Arabian Gulf seabed and the Heavy Metals Analysis Laboratories in the Nuclear Technologies Institute (NTI) at KACST for measuring the concentrations of targeted heavy metals for this research. The authors extend their sincere thanks to Khaled S. Alharbi, Mohammed F. Alotaibi, Mohammed S. Almoiqli, and Muath A. Alkadi for their contribution to preparing the soil samples for analysis and treatment.

References

- ASTM D2487, 2011. Standard practice for classification of soils for engineering purposes (Unified Soil Classification System). American Society for Testing and Materials, Philadelphia, USA.
- ATSDR (Agency for Toxic Substances and Disease Registry), 2022. Toxicological profiles for selected metals. U.S. Department of Health and Human Services.
- Al-Darwish, M., Yassen, B., 2005. Heavy metal accumulation in sediments and marine organisms from the Gulf of Oman. *Environ Monit Assess* 107, 75–92. <https://doi.org/10.1007/s10661-005-2017-z>
- Amin, S. A., Almahasheer, H. 2022. Pollution indices of heavy metals in the Western Arabian Gulf coastal area. *Egyptian Journal of Aquatic Research*, 48, 21–27. <https://doi.org/10.1016/j.ejar.2021.10.002>
- Birth, G.A. 2003. A Scheme for Assessing Human Impacts on Coastal Aquatic Environments Using Sediments. Woodcoffe, C.D. and Furness, R.A., Eds., Coastal GIS 2003, Wollongong University Papers in Centre for Maritime Policy, 14, Wollongong University Papers in Center for Maritime Policy, Australia.
- Cai, L., Xu, Z., Ren, M., Guo, Q., Hu, X., Hu, G., Peng, P., 2019. Source identification and risk assessment of heavy metals in surface sediments from the Pearl River Estuary, China. *Environ Pollut* 245, 414–424. <https://doi.org/10.1016/j.envpol.2019.11.006>

- Elgendy, M. Y., Al-Qahtani, A., & Al-Sorogy, A. S. (2024). Spatial distribution and ecological risk of heavy metals in coastal sediments of the Arabian Gulf. *Environmental Monitoring and Assessment*, 196, 732. <https://doi.org/10.1007/s10661-024-12906-8>.
- El-Sharkawy, M., Mahboob, S., & Al-Kahtany, A. (2025). Integrated Approaches for Coastal Pollution Control and Industrial Effluent Management. *Sustainability*, 16(5), 1921. <https://doi.org/10.3390/su16051921>
- EPA (U.S. Environmental Protection Agency). (2015). Regional Screening Levels (RSLs) for Chemical Contaminants. U.S. Environmental Protection Agency, Washington, DC. <https://www.epa.gov/esam/method-2007-determination-metals-and-trace-elements-water-and-wastes-inductively-coupled>
- Faisal, M., Salah-Tantawy, T., Al-Rashid, M., 2025. Integrated geochemical and ecological risk assessment of coastal sediments using multivariate approaches. *Mar Environ Res* 199, 106177.
- Forstner, U., Wittmann, G.T.W., 2012. *Metal pollution in the aquatic environment* (2nd ed.). Springer, Berlin. <https://doi.org/10.1007/978-3-642-69385-4>
- Hakanson, L., 1980. An ecological risk index for aquatic pollution control: a sedimentological approach. *Water Res* 14, 975-1001. [https://doi.org/10.1016/0043-1354\(80\)90143-8](https://doi.org/10.1016/0043-1354(80)90143-8)
- He, J., Zhang, Y., Zhang, M., 2020. Relationship between sediment grain size and heavy metal accumulation in coastal systems. *J Soils Sediments* 20, 3211-3223.
- Jupp, B.P., Al-Mutairi, M.S., Hasan, M., 2023. Geochemical assessment of metal pollution in Kuwait Bay sediments. *Environ Earth Sci* 82, 124. <https://doi.org/10.1007/s12665-023-10827-0>
- Long, E.R., Macdonald, D.D., Smith, S.L., Calder, F.D., 1995. Incidence of adverse biological effects within ranges of chemical concentrations in marine and estuarine sediments. *Environ Manage* 19, 81-97. <https://doi.org/10.1007/bf02472006>
- MacDonald, D.D., Ingersoll, C.G., Berger, T.A., 2000. Development and evaluation of consensus-based sediment quality guidelines for freshwater ecosystems. *Arch Environ Contam Toxicol* 39, 20-31. <https://doi.org/10.1007/s002440010075>
- Mahboob, S., Al-Ghanim, K., Al-Balawi, H., 2022. Heavy metal concentrations and ecological risk assessment in sediments from Abu Ali Island, Arabian Gulf. *Marine Pollution Bulletin* 178, 113627. <https://doi.org/10.1016/j.marpolbul.2021.101677>
- Mohamed, A., Al-Yami, H. M., Naser, H.A., 2024. Biological responses to sediment metal contamination in Arabian Gulf benthic fauna. *Ecotoxicol Environ Saf* 273, 115024. <https://doi.org/10.1016/j.ecoenv.2024.115024>
- Müller, G., 1969. Index of geoaccumulation in sediments of the Rhine River. *Geojournal* 2, 108-118. <https://ci.nii.ac.jp/naid/10030367619>
- Naser, H.A., 2013. Assessment and management of heavy metal pollution in the Arabian Gulf: A review. *Marine Pollution Bulletin* 72, 6-13. <https://doi.org/10.1016/j.marpolbul.2013.04.030>
- Que, W., Yi, L., Wu, Y., Li, Q. 2024. Analysis of heavy metals in sediments with different particle sizes and influencing factors in a mining area in Hunan Province. *Sci Rep* 14, 20318. <https://doi.org/10.1038/s41598-024-71502-3>
- Salah-Tantawy, T., Faisal, M., Al-Rashid, M., 2025. Integrating geochemical indices and multivariate statistics for ecological risk evaluation of marine sediments. *Environ Sci Pollut Res* 32, 41251-41266.
- Singh, K.P., Malik, A., Mohan, D., Sinha, S., 2004. Multivariate statistical techniques for the evaluation of spatial and temporal variations in water quality. *Water Res* 38, 3980-3992. <https://doi.org/10.1016/j.watres.2004.06.011>
- Suresh, G., Sutharsan, P., Ramasamy, V., Venkatachalapathy, R., 2012. Assessment of spatial distribution and potential ecological risk of heavy metals in sediments from the Gulf of Mannar, India. *Marine Pollution Bulletin* 64, 75-80. <https://doi.org/10.1016/j.ecoenv.2012.06.027>
- Sutherland, R.A., 2000. Bed sediment-associated trace metals in an urban stream, Oahu, Hawaii. *Environ Geol* 39, 611-627. <https://doi.org/10.1007/s002540050473>
- Swarnakar, S., Das, S., Chakraborty, P., 2024. Sediment contamination and ecological risk assessment in coastal environments. *Marine Pollution Bulletin* 193, 114997. <https://doi.org/10.1016/j.marpolbul.2024.114997>
- Swetha, S., Veerasingam, S., Rajendran, S., Hassan, H., Rahman Hashmi, M.U.R., Alsaadi, H., Rangel-Buitrago, N., Sadooni, F. N. 2025. Long-term trends in heavy metal contamination of marine sediments in the Arabian Gulf: A meta-analysis. *Environ Monit Assess* 197, 873. <https://doi.org/10.1007/s10661-025-14348-0>
- Taylor, S.R., McLennan, S.M., 1995. The geochemical evolution of the continental crust. *Rev Geophys* 33, 241-265. <https://doi.org/10.1029/95rg00262>
- Tomlinson, D.L., Wilson, J.G., Harris, C.R., Jeffrey, D.W., 1980. Problems in the assessment of heavy-metal levels in estuaries and the formation of a pollution index. *Helgolander Meeresunters* 33, 566-575. <https://doi.org/10.1007/bf02414780>
- Turekian, K.K., Wedepohl, K.H., 1961. Distribution of elements in some major units of the Earth's crust. *Geological Society of America Bulletin* 72, 175-192. [https://doi.org/10.1130/0016-7606\(1961\)72\[175:DOTAIS\]2.0.CO;2](https://doi.org/10.1130/0016-7606(1961)72[175:DOTAIS]2.0.CO;2)
- Varol, M., 2011. Assessment of heavy metal contamination in sediments of the Tigris River (Turkey) using pollution indices and multivariate statistical techniques. *J Hazard Mater* 195, 355-364. <https://doi.org/10.1016/j.jhazmat.2011.08.051>
- Zhang, J., Liu, C. L. 2002. Riverine Composition and Estuarine Geochemistry of Particulate Metals in China—Weathering Features, Anthropogenic Impact and Chemical Fluxes. *Estuarine, Coastal and Shelf Science*, 54, 1051-1070. <https://doi.org/10.1006/ecs.2001.0879>
- Zhang, Z., Juying, L., Mamat, Z., Qing, F.Y. (2016). Sources identification and pollution evaluation of heavy metals in the surface sediments of Bortala River, Northwest China. *Ecotox Environ Safe* 126, 94-101. <https://doi.org/10.1016/j.ecoenv.2015.12.025>